Title

Direct Visualization of the Binding of Transforming Growth Factor Beta 1 with Cartilage Oligomeric Matrix Protein via High-Resolution Atomic Force Microscopy

Journal

The Journal of Physical Chemistry B, 124(43)

ISSN

1520-6106

Authors

Tran, Victoria
Karsai, Arpad
Fong, Michael C
et al.

Publication Date

2020-10-29

DOI

10.1021/acs.jpcb.0c07286

Peer reviewed

Published in final edited form as:

J Phys Chem B. 2020 October 29; 124(43): 9497–9504. doi:10.1021/acs.jpcb.0c07286.

Direct Visualization of the Binding of Transforming Growth Factor Beta 1 with Cartilage Oligomeric Matrix Protein via High-Resolution Atomic Force Microscopy

Victoria Tran[1], **Arpad Karsai**[1], **Michael C. Fong**[2], **Weiliang Cai**[3], **J. Gabriel Fraley**[3], **Jasper H.N. Yik**[3], **Eric Klineberg**[3], **Dominik R. Haudenschild**[3], **Gang-yu Liu**[1,*]

[1]Department of Chemistry, University of California, Davis, CA, 95616, United States

[2]Department of Biomedical Engineering, University of California, Davis, CA, 95616, United States

[3]Department of Orthopaedic Surgery, University of California-Davis Medical Center, Sacramento, CA, 95817, United States

Abstract

This work reports the first direct observations of binding and complex formation between transforming growth factor beta 1 (TGF-β1) and cartilage oligomeric matrix protein (COMP) using high-resolution atomic force microscopy (AFM). Each COMP molecule consists of pentamers whose five identical monomeric units bundle at N-termini. From this central point, the five monomers' flexible arms extend outward with C-terminal domains at the distal ends, forming a bouquet-like structure. In commonly used buffer solutions, TGF-β1 molecules typically form homodimers (majority), double dimers (minority), and aggregates (trace amount). Mixing of TGF-β1 and COMP leads to rapid binding and complex formation. The TGF-β1/COMP complexes contain one to three COMP and multiple TGF-β1 molecules. For complexes with one COMP, the structure is more compact and less flexible than that of COMP alone. For complexes with two or more COMP molecules, the conformation varies to a large degree from one complex to another. This is attributed to the presence of double dimers or aggregates of TGF-β1 molecules, whose size and multiple binding sites enable binding to more than one COMP. The number and location of individual TGF-β1 dimers are also clearly visible in all complexes. This molecular-level information provides new insight into the mechanism of chondrogenesis enhancement by TGF-β1/COMP complexes, i.e. simultaneous and multivalent presentation of growth factors. These presentations help explain the high efficacy in sustained activation of the signalling pathway to augment chondrogenesis.

Graphical Abstract

[*]**Authors to whom correspondence should be addressed** Gang-yu Liu, Ph.D., Department of Chemistry, University of California, Davis, CA 95616, Phone: (530) 754-9678, Fax:(530) 754-8557, gyliu@ucdavis.edu.

AUTHOR DISCLOSURE STATEMENT

None of authors has competing interests.

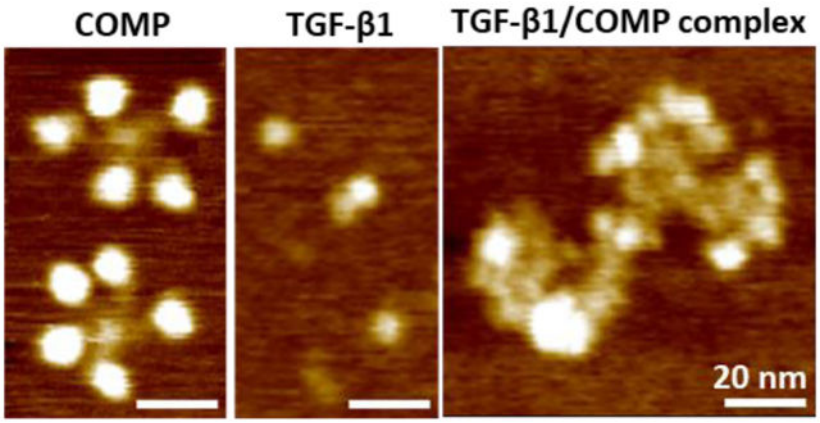

1. INTRODUCTION

Transforming growth factor beta 1 (TGF-β1) belongs to a superfamily of multifunctional growth factors that regulate a variety of biological functions including cell proliferation, differentiation, and maturation.[1, 2] It has been implicated as an important regulatory molecule during differentiation of mesenchymal stem cells (MSC) into chondrocytes for cartilage formation.[1] Recent studies have suggested that the manner in which growth factors are presented to cell surface receptors is vital for regulating and enhancing differentiation.[3, 4] Prior investigation by our team discovered that the mixtures of TGF-β1 with cartilage oligomeric matrix protein (COMP), an extracellular matrix component, elicited a greater enhancement on the signalling transduction activity than TGF-β1 alone.[5] COMP (524 kDa) is a disulfide-bonded homo-pentameric glycoprotein found in the extracellular matrix of cartilage, tendons, bone tissue, and ligaments.[6, 7] Its structure is composed of five identical monomers, each consisting of an N-terminal coiled-coil domain, four epidermal growth factor (EGF) repeats, eight thrombospondin-3 repeats, and a C-terminal domain.[8, 9] The pentameric structure of COMP allows its simultaneous interaction with multiple entities such as growth factors,[4, 5, 10] fibronectin,[11] and collagen.[12] Thus, COMP is recognized as a potential scaffold to coordinate the presentation of multiple growth factors to cells. For example, it was postulated that COMP and TGF-β1 formed complexes, and as such, enabled multi-valent presentation of growth factors and enhanced chondrogenesis.[5] However, the precise molecular interaction is not completely understood, such as the occupancy of growth factor binding sites on COMP. Hence, it is important to acquire molecular-level knowledge of the binding and conformation of each growth factor molecule in the complex, as the growth factor presentation directly impacts its subsequent interactions with cells, and the cellular signalling processes downstream.

Prior attempts to image these complexes included negative stained transmission electron micrograph (TEM) using colloidal thiocyanate gold nanoparticle labelled TGF-β1 in conjunction with protein fixation and uranyl formate stains.[5] However, the impact of labels and treatments on the reactivities and structural integrity remains unknown. Therefore, a label-free technology with the capability of imaging protein in buffer media is needed. Atomic force microscopy (AFM), known for being label-free, high-resolution and versatile,

provides a powerful tool to fill the void. In fact, AFM has been utilized to image a variety of biological specimens including cells, proteins, and DNA at nanometre resolution.[13-20] AFM enables protein molecules to be visualized in buffer with nanometre resolution in three-dimensions.[21-26] In fact, our prior work has demonstrated that AFM enabled high-resolution imaging of BMP-2/COMP complexes.[4] This work utilizes AFM to investigate the COMP and TGF-β1 systems to reveal the binding and structure of the complexes. The measured outcomes include direct observation of the proteins, and protein complex formation including TGF-β1 molecules within each complex. These observations provide a molecular level insight into growth factor binding behaviour and the mechanism for their enhancement of chondrogenesis.

2. EXPERIMENTAL SECTION

2.1. Materials Used for this investigation.

HEPES (1M), hydrochloric acid (36.5–38.0% w/w), and TRIS (Base) were ordered from Fisher Scientific (Hampton, NH). Phosphate-buffered saline (PBS) (1X) was purchased from Mediatech (Manassas, VA). Sodium chloride, NaCl, (≥99%), and calcium chloride, $CaCl_2$ (≥96%) were all purchased from Sigma-Aldrich (St. Louis, MO). Deionized water with a resistivity of 18.2 MΩ·cm was generated using a Millipore Milli-Q system (EMD Millipore, Billerica, MA). Mica sheets were purchased from S & J Trading INC (Glen Oaks, NY). Amicon Centrifugal Filter Unit with 100 kDa molecular weight cut-off (catalog #: UFC910024) was purchased from Millipore Sigma (Burlington, MA).

2.2. Recombinant human COMP and TGF-β1.

Recombinant human COMP was expressed and purified as described previously.[5] Briefly, the COMP expression cassette was cloned into a pCCL3 lentiviral vector and transfected into human 293T cells (American Type Culture Collection, Manassas, VA) in serum-free culture medium. Recombinant human COMP was purified from the cell culture medium to near homogeneity via nickel-NTA column affinity chromatography. After purification the buffer exchange was done using Amicon Centrifugal Filter Unit with 100 kDa molecular weight cut-off and the sample was concentrated to the desired concentration, typically 860 nM, using the same filter unit. Purified COMP was stored in 20 mM HEPES buffer (pH 7.0), 500 mM NaCl, and 2 mM $CaCl_2$ at 4 °C[27] Human TGF-β1 was purchased from PeproTech (Rocky Hill, NJ). Solid, white powder TGF-β1 was resuspended in 4 mM HCl to obtain a stock concentration of 7700 nM.

2.3. Protein immobilization on mica(0001) surfaces.

Protein immobilization followed our prior protocol.[4] Stock solution of COMP (860 nM) was diluted with 20 mM HEPES buffer, pH 6.8, 100 mM NaCl and 2 mM $CaCl_2$ to a working concentration of 2 nM. A volume of 100 μl of protein solution was deposited onto a freshly cleaved mica(0001) surface. After 2 minutes of absorption, the mica surface was washed with ultra-pure Milli-Q water (18.2 MΩ.cm) to remove loosely attached proteins and buffer residues. The samples were dried by gently blowing clean compressed air onto mica surfaces before AFM imaging. Immobilization of TGF-β1 followed the same protocols. Stock

solution of TGF-β1 (7700 nM) was diluted with 20 mM HEPES buffer, pH 6.8, 100 mM NaCl and 2 mM $CaCl_2$ to reach a working concentration of 20 nM.

The TGF-β1/COMP complex was formed by pre-mixing COMP and TGF-β1 for 1 hour at room temperature in 20 mM HEPES buffer, pH 6.8, 100 mM NaCl and 2 mM $CaCl_2$ before deposition. The concentration of COMP and TGF in the solution was 2 nM and 20 nM respectively. The pH of the binding buffers was set at 6.8 to ensure optimal binding of TGF-β1 to COMP.[5] Following the same procedures of protein deposition as described above, the protein complexes were immobilized onto freshly cleaved mica (0001) surfaces, washed with ultrapure water and dried with compressed air. Samples were imaged immediately after drying.

For the concentration-dependent experiment, COMP and TGF-β1 were mixed in 50 mM Tris-buffered saline (TBS), pH 6.8, 150 mM NaCl and 16 mM $CaCl_2$. The concentration of TGF-β1 varied from 2-40 nM while maintaining the concentration of COMP constant at 2nM. A similar protocol as above was applied for immobilization of the mixture on the mica(0001) surface.

2.4. Atomic force microscopy.

Atomic force microscopy (AFM) images were acquired using a commercial instrument (MFP-3D, Oxford instrument, Santa Barbara, CA). Tapping mode and soft cantilevers were utilized to minimize perturbation to the immobilized protein molecules on surfaces.[13, 16] All images were taken using MSNL-10 cantilevers (Bruker Nano, Camarillo, CA) with a force constant of 0.6 N/m and resonant frequency of 109 kHz. For tapping mode imaging under ambient conditions, the driving frequency, drive amplitude and damping were set at 109 kHz, 0.30V and 25% respectively. Data acquisition were carried out using MFP-3D software developed based on the Igor Pro 6.12 platform.

3. RESULTS

3.1. High-Resolution AFM Images Reveal the Formation of the TGF-β1/COMP Complexes upon Mixing.

We investigated the interaction of TGF-β1 and COMP by comparing high-resolution AFM images of the COMP, TGF-β1, and their mixtures after immobilization onto mica(0001) surfaces. Mica(0001) surfaces were chosen as the support because they are atomically flat structures.[4, 22, 28, 29] In Figure 1, the characteristic AFM topographical images for all three systems are displayed side-by-side, using the same scanning size of 500 x 500 nm^2

In Figure 1A, 100 βl of 2 nM COMP solution was deposited onto mica(0001) for 2 minutes, followed by washing with milli-Q water and drying with compressed air before AFM imaging. Individual COMP molecules were clearly separated and visualized. Each COMP adopts its individual conformation that can be described as a “gecko’s foot”. This morphology is characteristic of a viable COMP molecule in buffer, as reported in our prior studies.[4] The globular end of each gecko finger appears brighter, i.e., taller than the arm, corresponding to the C-terminal domain. The orientation of each monomer within the pentameric COMP is also clearly visualized under AFM imaging. Consistent with prior

reports, COMP molecules exist as a homo-pentameric glycoprotein composed of five identical units assembling together with N-termini at the centre and C-termini at the distal end.[4, 30-32] Molecules exhibited various conformations upon immobilization owing to the flexibility of its monomer arms and assembly.[4, 5, 30] The AFM morphology of COMP molecules is also consistent with prior X-ray crystallography of two truncated COMP and prior TEM studies of pentameric COMP, in which the N-termini of pentameric COMP bundles at the center while the C-terminus extends outward.[5, 9, 27, 32]

In Figure 1B, 100 μl of 20 nM TGF-β1 solution was pipetted onto mica(0001) for 2 minutes and then washed and dried prior to AFM imaging. Each bright "bump" corresponds to TGF-β1 molecules. It is known that TGF-β1 molecules exist as homodimers,[33, 34] thus one would anticipate uniform sized features in AFM topography. However, Figure 1B reveals variation of the feature size, therefore, we suspected that TGF-β1 under these conditions might have formed aggregates. The aggregation status has been analysed in detail under higher-resolution imaging as discussed in the next section.

Upon mixing TGF-β1 and COMP for 1 hour, the mixture of TGF-β1 and COMP was then deposited onto mica(0001) following the same protocol as Figure 1A and 1B. The outcome, shown in Figure 1C, clearly reveals new features whose morphology significantly differs from either that of COMP or TGF-β1 alone. This is a direct and clear indication that binding occurred and TGF-β1/COMP complexes formed. From the size and overall morphology, the features can be categorized into two groups (a) complexes containing one COMP molecule and multiple TGF-β1 molecules (e.g. arrow 1); and (b) complexes containing two or more COMP molecules and multiple TGF-β1 molecules (e.g. arrows 2 and 3). The complexes containing one COMP adopt a geometry that can be described as a "sea otter paw" (arrow 1). The complexes containing two COMP molecules adopt various conformations, e.g., the geometries of a "butterfly" (arrow 2), and a "sting ray" (arrow 3). This finding is rational as the variation in molecular conformation increases with its size and complexity.

3.2. High-Resolution AFM Images Reveal Aggregation Status of TGF-β1 Molecules.

Figure 2A shows TGF-β1 molecules from an aqueous solution containing 20 mM HEPES buffer (pH 6.8), 100 mM NaCl, and 2 mM $CaCl_2$. Under this condition, the TGF-β1 molecules have positive net charge of +8, which was determined using the Prot pi calculator.[35] Upon immobilization onto a mica(0001) surface, AFM imaging were acquired using tapping mode. The bright features in Figure 2A are attributed to TGF-β1 molecules. These features are well separated, yet vary in size, thus likely the results of various aggregations of TGF-β1 molecules in the solution. As TGF-β1 and bone morphogenetic protein-2 (BMP-2) are from the same TGF-β superfamily, we expect that the dimer form of these proteins would be comparable. The smallest features of TGF-β1 molecules, as shown in the green inset example, measures 6.4 nm wide, 7.5 nm long, and 1.0 nm tall (cursor, Figure 2B). These measurements are similar to that of BMP-2 dimers (7.5 ± 1.3 nm wide, 10.0 ± 2.0 nm long, and 0.8 ± 0.1 nm tall) under AFM imaging in ambient conditions. Therefore, these smallest features are consistent with TGF-β1 dimers immobilized with molecular axis parallel to mica surface, i.e. belly down, as illustrated via the protein model in Figure 2B. TGF-β1 dimers represents 41% of the protein population in the solution. The next size up,

e.g., in the blue inset, measures 10.3 nm wide, 11.7 nm long, and 1.3 nm tall (cursor, Figure 2C), almost twice in volume as that the TGF-β1 dimers, which are consistent with a double dimer. The double dimer represents 16% of the TGF-β1 population. Large aggregates are also present, for example, the purple inset measures 12.9 nm x 14.5 nm x 2.3 nm (cursor, Figure 2D). These aggregates make up 23% of the protein populations. The other 20% of the TGF-β1 population are between double dimer and aggregate of dimers in size. In contrast to BMP-2 solutions, which contain near 100% dimers,[4] TGF-β1 molecules in solution exhibit dimers, double dimers, aggregations, i.e. heterogeneity in aggregation status in standard buffer solutions (20 mM HEPES buffer, pH 6.8, 100 mM NaCl, and 2mM $CaCl_2$). These observations were reproducible among all five independent experiments, each imaged with multiple randomly selected areas. As will be discussed in detail in later sections, the aggregation leads to complexity and rich structures in TGF-β1/COMP binding.

3.3. High-Resolution AFM Images Reveal Structural Details within the TGF-β1/COMP Ccomplexes.

While we concluded from Figure 1 that binding occurred when mixing TGF-β1 and COMP, additional structural information requires a zoom-in view of protein molecules. Figure 3 shows representative high-resolution images of the protein systems under this investigation. Figure 3A displays the characteristic pentameric structure of COMP molecules, to which the complex images will be compared to reveal binding information. Immobilized COMP molecules were also images in buffer solutions. The morphology and apparent height measurements are very similar to that shown in Figures 1A and 3A. A TGF-β1 dimer and a double dimer are displayed in Figure 3B, whose dimensions provides a guide to identify the location of TGF-β1 molecules in the TGF-β1/COMP complexes.

Figure 3C shows a TGF-β1/COMP complex containing one COMP molecule. This complex exhibits a geometry like that of a “sea otter paw”, with 5 “toes” at the top of the periphery. Four out of the five toe-like features are assigned as the TGF-β1 molecules (arrows). Key evidence arises from the disappearance of the C-terminal domains of COMP in those arms, and the comparison of topographic dimensions with that in Figure 3B. The C-terminal domains of COMP undergo a conformational change to bind growth factor molecules.[4] The bright domain on the right is like due to the remaining arm of COMP not reacting with TGF-β1. In this complex, 3 out of 5 arms of the COMP are bound to 3 TGF-β1 dimers (thin arrows), respectively, and 1 arm (right) is bound to a TGF-β1 double dimer (thick arrow). Comparing Figure 3A with Figure 3C, it is evident that the TGF-β1/COMP complex exhibits a more compact structure than that of a COMP molecule: monomer arms of COMP are well spread, while arms of the TGF-β1/COMP are hardly recognizable. The compactness can be estimated quantitatively from the AFM topography by taking the ratio of occupied area over the total footprint area: 68% for a COMP shown in Figure 3A, versus 98% in Figure 3C. The compactness of the complex could explain its lower flexibility than that of COMP.[4]

Figure 3D shows another TGF-β1/COMP complex, whose geometry resembles that of a “butterfly”. The footprint of this complex is almost 1.5X as large as that in Figure 3C, thus we infer that two COMP molecules participated in the reaction. Nine TGF-β1 binding sites

can be clearly visualized, scattered around the complex, as indicated by arrows. Comparing its size with that in Figure 3B, these sites consist of 7 TGF-β1 dimers (arrows) and 1 double dimer (thicker arrow at lower right). The 2 bright features atop of the two butterfly wings are consistent with the C-terminal domains in COMP, thus are assigned to the unbound sites. This complex is also more compact than that of COMPs, estimated to be 77% in comparison to the 68% of the COMP. Although appearing small, the TGF-β1 site in the middle of butterfly joining the two COMPs, is likely a double-dimmer, whose location and orientation are so well-inlaid that only a small portion is visible under AFM. The binding sites in each TGF-β1 double dimer are twice as many as that in a dimer. The longest binding site separation in the double dimer is also larger than that in a single dimer. Therefore, the chance for a double dimer to capture 2 COMP molecules is enhanced. In addition to the sea-otter paw and butterfly conformation, other conformations of TGF-β1/COMP complex are also captured faithfully by AFM, e.g. a “stingray” as indicted by arrow 3 in Figure 1C. Because of the size and complexity of the complexes containing 2 COMPs, conformations vary to a larger degree than complexes containing a single COMP. These observations were reproducible in all 5 independent experiments, each imaged with multiple randomly selected areas.

3.4. Structure and Conformation of TGF-β1/COMPcomplexes Vary with Increase of TGF-β1 Concentration.

Using the same COMP concentration (2 nM) as the experiment shown in Figure 1, we increased the concentration of TGF-β1 from 2 to 40 nM, as such, the molar ratio of COMP:TGF-β1 decreased from 1:1 to 1:20. Figure 4 compares the trend of the formation of the complex with the decreasing of COMP:TGF-β1 ratio.

The effect of molar ratio of COMP:TGF-β1 on unbound TGF-β1 molecules were clearly seen when comparing Figures 4A-4D. Two trends were observed: the number of unbound TGF-β1 molecules increased with increasing of TGF-β1 concentration or decreasing of COMP:TGF-β1 ratio, and more and more unbound double dimers and aggregates appeared as well. Focusing on the areas without the complexes: at ratio of 1:1, two TGF-β1 dimer molecules were clearly visible in Figure 4A. When the ratio was decreased to 1:5 (Figure 4B), there were almost 6X unbound and free TGF-β1 dimers as that in Figure 4A. Not only were TGF-β1 dimers present, but 14 small clustering of TGF-β1 dimers, e.g. double dimers and aggregates, were seen. At ratio of 1:10, 6 individual TGF-β1 dimers, and 22 TGF-β1 double dimers and aggregates were observed in Figure 4C. The amount of unbound TGF-β1 double-dimmers and aggregates doubled in comparison to Figure 4B. The trends continue, in Figure 4D at 1:20 ratio, there were 12 TGF-β1 dimers, and 36 double dimers and aggregates, respectively.

Three trends regarding the TGF-β1/COMP complexes were clearly observed comparing all images in Figure 4 from left to right. *First*, the population of complexes containing 2 COMPs increased approximately 2X the amounts as the COMP:TGF-β1 ratio decreased to 1:20. For each sample, at least 8 images were acquired, from which we counted the number of complexes containing 2 COMPs versus the total populations. At a 1:1 ratio (e.g. Figure 4A), the majority of the population of the complex contains one COMP, only 13% ± 3% of

the population contained 2 COMPs, which was taken from 8 number of images in this investigation. At a ratio of 1:5 (e.g Figures 4B), the complex population containing 2 COMPs reaches 15% ± 5%. At a ratio of 1:10 (e.g. Figure 4C), 10% ± 5% of the population contained 2 COMPs. Decreasing the ratio to 1:20 (e.g. Figure 4D), 23% ± 5 % complexes had 2 COMPs, which is approximately 2X as that in Figure 4A. Though the population of complexes containing 2 COMPs does not increase with the ratio of COMP:TGF-β1, it is evident that the formation of 2 COMP complexes increase with more TGF-β1.

Second, comparing complexes containing one COMP, the number of TGF-β1 molecules per complex increased with increasing TGF-β1 concentration. In Figure 4A1 with COMP:TGF-β1 ratio of 1:1, two TGF-β1 molecules were clearly seen (yellow arrows), while the other 3 monomer units in COMP did not participate in binding, as characterized by the bright C-terminal domains (red arrows). The apparent height of these C-termini measured as 1.9 ± 0.2 nm, consistent with the known AFM topography of COMP.[4] Decreasing the ratio to 1:5, Figure 4B1 shows that 3 TGF-β1 molecules bound to COMP, and only 2 unbound arms remained. At the ratio of 1:10, the characteristic “gecko’s foot” conformation of COMP completely vanished, and the complex exhibited a more compact conformation of “sea otter paw”, as shown in Figure 4C1. Four TGF-β1 molecules are clearly visible, but we infer 5 binding events from the lack of C-terminal domains in Figure 4C1. At ratio of 1:20, at least 6 TGF-β1 molecules could be clearly identified in the complex shown in Figure 4D1, which is more than the conventional view of 5 binding sites per COMP. The presence of TGF-β1 double dimers and aggregates is attributed to the observations of >5 TGF-β1 dimers/COMP.

Third, for complexes containing 2 COMP molecules, the number of TGF-β1 molecules per complex increased with the decreasing of COMP:TGF-β1 ratio. We note that not all TGF-β1 dimers could be captured in those cases due to the complexity in the conformation and binding location, e.g. growth factors were only partly exposed or completely hidden from outmost surfaces. Therefore, the TGF-β1 dimers identified from AFM images represent the minimum number of binding events. At 1:1 ratio, shown in Figures 4A2, at least 3 TGF-β1 molecules were visible (yellow arrows), while 6 monomers in the COMP remain unbound (red arrows). At 1:5 ratio, the complex in Figure 4B2 contained at least 4 TGF-β1 dimers. The number of TGF-β1 binding event increased to 10 in Figure 4C2, at the ratio of 1:10. At COMP:TGF-β1 = 1:20, the number of TGF-β1 per complex increased further, as shown in Figure 4D2, where at least 13 TGF-β1 dimers were clearly visualized. These observations demonstrate the robustness of our conclusion that TGF-β1/COMP complexes formed upon mixing and suggest that double dimers and aggregates of TGF-β1 were responsible for the formation of large complexes (i.e. more than 1 COMP) and large numbers of TGF-β1 dimers in these complexes.

4. DISCUSSION

It is known that each COMP molecule has 5 high affinity binding sites for growth factors such as TGF-β1 and BMP-2.[5, 6, 10] Prior studies have shown that binding likely occurs in the C-terminal region (~200 residues) using hybrid β-galactosidase and in-vitro GST pull-down assays.[27, 36] TGF-β1 and BMP-2 belong to the transforming growth factor super-family, and likely bind to the general C-terminal region of COMP.[5, 6, 37, 38] In fact, our past and current

investigations revealed similarities among TGF-β1/COMP and BMP-2/COMP binding: (a) C-terminal domains of COMP, which are typically taller than the chain due to folded conformation undergo a conformation change due to binding of growth factors; and (b) the complexes are more densely packed and less flexible than COMP, as illustrated in Figure 5. We describe COMP geometry as “gecko’s foot” which is flexible and spread out. By comparison, TGF-β1/COMP and BMP-2/COMP complexes reassemble “sea otter paw” and “gummy bear”, respectively.

Figure 5 also illustrates key differences between TGF-β1 and BMP-2 in the context of their binding with COMP. Almost all BMP-2/COMP complexes contain only 1 COMP per complex, exhibiting various of “gummy bear” morphologies under AFM imaging, as shown in Figure 5A. In contrast, the majority of TGF-β1/COMP complexes contain 1 COMP per complex, but some TGF-β1/COMP complexes contain 2 or more COMPs, as illustrated in Figure 5B. These large complexes exhibit a wider range of conformations, e.g. “butterfly”, or “sting ray”. As illustrated in Figure 5B, the formation of these large complexes is attributed to the double dimers or aggregates of TGF-β1 molecules, whose size and multiple binding sites enable binding to more than one COMP.

Another difference arises from the observation that TGF-β1 molecules in the complexes appear taller and more clearly resolved than that of BMP-2 molecules. We attribute this observation to the differences in molecular dimension and their binding behaviour to COMP. The geometry and dimensions of TGF-β1 and BMP-2 dimers can be found from the PDB and are compared in Figure 5.[38, 39] Clearly, TGF-β1 is physically larger than BMP-2, thus more visible in AFM topographs. In addition, BMP-2 dimers are likely more inlaid in the binding pockets of COMP than those of TGF-β1 dimers, i.e. the presentation of TGF-β1 is more “exposed”.

While TGF-β1 and BMP-2 belong in the same TGF superfamily and have a relatively similar structure, they exhibit characteristic differences in their binding interactions with their respective receptors.[6, 38] TGF-β1 binds only to Type I (TβR-I) and Type II (TβR-II) receptors, while BMP-2 can interact with two Type I (Alk1, Alk2) and three Type II (ActR-II, ActR-IIb BMPR-II) receptors.[38] Our observed differences of BMP-2 and TGF-β1 binding behaviour to COMP also help rationalizing their different interactions with these receptors. Prior investigations by our team reported that the mixtures of TGF-β1 with COMP elicited a greater enhancement on the signalling transduction activity than TGF-β1 alone.[5] We infer that the presentation of TGF-β1 molecules in the TGF-β1/COMP complexes expose the binding domains to receptors, and allow simultaneous and multivalent binding to receptors. The multivalent presentations led to high efficacy in sustained activation of the signalling pathway to augment chondrogenesis. Other signalling processes could also be impacted by the presentation of growth factors. Recent studies have suggested that the manner in which growth factors are presented to the cell receptors are vital for regulating and enhancing differentiation.[3]

5. CONCLUSIONS

This work presents the first direct observations of binding and complex formation between TGF-β1 and COMP molecules using high-resolution AFM imaging. Exploiting the high spatial resolution and label-free nature of AFM, this investigation indicated that TGF-β1 molecules exhibit as homodimers (majority), double dimers, and aggregates in commonly used buffers (e.g. pH = 6.8 and 20 mM HEPES buffer with 100 mM NaCl, and 2mM $CaCl_2$). Individual COMP molecules adopt a pentameric structure whose five identical monomer units bundle at N-termini. From this central point, the five flexible monomer chains extend to C-terminal domains at the distal ends, whose conformations are bulkier than the chains. Mixing COMP and TGF-β1 in buffer led to formation of complexes quickly in room temperatures. The TGF-β1/COMP complexes contain one to three COMP and multiple TGF-β1 dimers. For complexes with one COMP, the structure is more compact and less flexible than that of COMP alone. For complexes with two or more COMP molecules, the conformation varies significantly from one complex to another. The formation of these large complexes is attributed to the double dimers or aggregates of TGF-β1 molecules, whose sizes and multiple binding sites enable binding to more than one COMP. The formation of large complexes occurred more frequently in the case of TGF-β1 and COMP binding, in contrast to that of BMP-2 and COMP. The number and location of individual TGF-β1 dimers are also clearly visible in the TGF-β1/COMP complexes. In most cases, 1-5 TGF-β1 dimers per COMP were seen among complexes, consistent with the knowledge that each COMP contains 5 strong binding sites to growth factors. In some cases, more than 5 TGF-β1 dimers per COMP were seen. The formation of large complexes and binding with more than 5 TGF-β1 dimers per COMP represent another key difference from that of BMP-2/COMP complexes. This molecular-level information provides new insight into the mechanism of chondrogenesis enhancement by TGF-β1/COMP complexes, i.e. simultaneous and multivalent presentation of growth factors. Revealing the multivalent presentation of TGF-β1 molecules deepens our understanding of the high efficacy in sustained activation of the signalling pathway to augment chondrogenesis.

ACKNOWLEDGMENT

This work was supported by UC Davis, the National Institutes of Health (R01-AR070239), Department of Defence (CDMRP-PR142010), National Science Foundation (CHE-1808829) and the Gordon and Betty Moore Foundation.

REFERENCE

1. Mizuta H; Sanyal A; Fukumoto T; Fitzsimmons JS; Matsui N; Bolander ME; Oursler MJ; O'Driscoll SW The Spatiotemporal Expression of Tgf-Beta 1 and Its Receptors During Periosteal Chondrogenesis in Vitro. J. Orthop. Res 2002, 20, 562–574. [PubMed: 12038632]
2. Clark DA; Coker R Transforming Growth Factor-Beta (Tgf-Beta). Int. J. Biochem. Cell Biol 1998, 30, 293–298. [PubMed: 9611771]
3. Re'em T; Kaminer-Israeli Y; Ruvinov E; Cohen S Chondrogenesis of Hmsc in Affinity-Bound Tgf-Beta Scaffolds. Biomaterials 2012, 33, 751–761. [PubMed: 22019120]
4. Tran V; Karsai A; Fong MC; Cai WL; Yik JHN; Klineberg E; Haudenschild DR; Liu GY Label-Free and Direct Visualization of Multivalent Binding of Bone Morphogenetic Protein-2 with Cartilage Oligomeric Matrix Protein. J. Phys. Chem. B 2019, 123, 39–46. [PubMed: 30554512]

5. Haudenschild DR; Hong E; Yik JH; Chromy B; Morgelin M; Snow KD; Acharya C; Takada Y; Di Cesare PE Enhanced Activity of Transforming Growth Factor Beta1 (Tgf-Beta1) Bound to Cartilage Oligomeric Matrix Protein. J. Biol. Chem 2011, 286, 43250–43258. [PubMed: 21940632]

6. Acharya C; Yik JH; Kishore A; Van Dinh V; Di Cesare PE; Haudenschild DR Cartilage Oligomeric Matrix Protein and Its Binding Partners in the Cartilage Extracellular Matrix: Interaction, Regulation and Role in Chondrogenesis. Matrix Biol. 2014, 37, 102–111. [PubMed: 24997222]

7. Hedbom E; Antonsson P; Hjerpe A; Aeschlimann D; Paulsson M; Rosapimentel E; Sommarin Y; Wendel M; Oldberg A; Heinegard D Cartilage Matrix Proteins - an Acidic Oligomeric Protein (Comp) Detected Only in Cartilage. J. Biol. Chem 1992, 267, 6132–6136. [PubMed: 1556121]

8. Efimov VP; Engel J; Malashkevich VN Crystallization and Preliminary Crystallographic Study of the Pentamerizing Domain from Cartilage Oligomeric Matrix Protein: A Five-Stranded Alpha-Helical Bundle. Proteins 1996, 24, 259–262. [PubMed: 8820492]

9. Malashkevich VN; Kammerer RA; Efimov VP; Schulthess T; Engel J The Crystal Structure of a Five-Stranded Coiled Coil in Comp: A Prototype Ion Channel? Science 1996, 274, 761–765. [PubMed: 8864111]

10. Ishida K; Acharya C; Christiansen BA; Yik JH; DiCesare PE; Haudenschild DR Cartilage Oligomeric Matrix Protein Enhances Osteogenesis by Directly Binding and Activating Bone Morphogenetic Protein-2. Bone 2013, 55, 23–35. [PubMed: 23528838]

11. Di Cesare PE; Chen FS; Moergelin M; Carlson CS; Leslie MP; Perris R; Fang C Matrix-Matrix Interaction of Cartilage Oligomeric Matrix Protein and Fibronectin. Matrix Biol. 2002, 21, 461–470. [PubMed: 12225811]

12. Blumbach K; Niehoff A; Paulsson M; Zaucke F Ablation of Collagen Ix and Comp Disrupts Epiphyseal Cartilage Architecture. Matrix Biol. 2008, 27, 306–318. [PubMed: 18191556]

13. Siedlecki CA; Marchant RE Atomic Force Microscopy for Characterization of the Biomaterial Interface. Biomaterials 1998, 19, 441–454. [PubMed: 9677156]

14. Dorn IT; Eschrich R; Seemuller E; Guckenberger R; Tampe R High-Resolution Afm-Imaging and Mechanistic Analysis of the 20 S Proteasome. J. Mol. Biol 1999, 288, 1027–1036. [PubMed: 10329196]

15. Hansma HG Atomic Force Microscopy of Biomolecules. J. Vac. Sci. Technol., B: Nanotechnol. Microelectron.: Mater., Process., Meas., Phenom 1996, 14, 1390–1394.

16. Fotiadis D; Scheuring S; Muller SA; Engel A; Muller DJ Imaging and Manipulation of Biological Structures with the Afm. Micron 2002, 33, 385–397. [PubMed: 11814877]

17. Hansma HG; Sinsheimer RL; Groppe J; Bruice TC; Elings V; Gurley G; Bezanilla M; Mastrangelo IA; Hough PVC; Hansma PK Recent Advances in Atomic-Force Microscopy of DNA. Scanning 1993, 15, 296–299. [PubMed: 8269178]

18. Wadu-Mesthrige K; Amro NA; Liu GY Immobilization of Proteins on Self-Assembled Monolayers. Scanning 2000, 22, 380–388. [PubMed: 11145264]

19. Liu GY; Amro NA Positioning Protein Molecules on Surfaces: A Nanoengineering Approach to Supramolecular Chemistry. Proc. Natl. Acad. Sci. U. S. A 2002, 99, 5165–5170. [PubMed: 11959965]

20. Tan YH; Liu M; Nolting B; Go JG; Gervay-Hague J; Liu GY A Nanoengineering Approach for Investigation and Regulation of Protein Immobilization. ACS Nano 2008, 2, 2374–2384. [PubMed: 19206405]

21. Patil S; Martinez NF; Lozano JR; Garcia R Force Microscopy Imaging of Individual Protein Molecules with Sub-Pico Newton Force Sensitivity. J. Mol. Recognit 2007, 20, 516–523. [PubMed: 17918769]

22. Viani MB; Pietrasanta LI; Thompson JB; Chand A; Gebeshuber IC; Kindt JH; Richter M; Hansma HG; Hansma PK Probing Protein-Protein Interactions in Real Time. Nat. Struct. Biol 2000, 7, 644–647. [PubMed: 10932247]

23. Bitler A; Lev N; Fridmann-Sirkis Y; Blank L; Cohen SR; Shai Y Kinetics of Interaction of Hiv Fusion Protein (Gp41) with Lipid Membranes Studied by Real-Time Afm Imaging. Ultramicroscopy 2010, 110, 694–700. [PubMed: 20399563]

24. Wang ZG; Zhou CQ; Wang C; Wan LJ; Fang XH; Bai CL Afm and Stm Study of Beta-Amyloid Aggregation on Graphite. Ultramicroscopy 2003, 97, 73–79. [PubMed: 12801659]

25. Valle F; DeRose JA; Dietler G; Kawe M; Pluckthun A; Semenza G Afm Structural Study of the Molecular Chaperone Groel and Its Two-Dimensional Crystals: An Ideal "Living" Calibration Sample. Ultramicroscopy 2002, 93, 83–89. [PubMed: 12380652]
26. Zykwinska A; Marquis M; Sinquin C; Marchand L; Colliec-Jouault S; Cuenot S Investigation of Interactions between the Marine Gy785 Exopolysaccharide and Transforming Growth Factor-Beta 1 by Atomic Force Microscopy. Carbohydr. Polym 2018, 202, 56–63. [PubMed: 30287036]
27. Tan K; Duquette M; Joachimiak A; Lawler J The Crystal Structure of the Signature Domain of Cartilage Oligomeric Matrix Protein: Implications for Collagen, Glycosaminoglycan and Integrin Binding. Fed. Am. Soc. Exp. Biol. J 2009, 23, 2490–2501.
28. Bergkvist M; Carlsson J; Karlsson T; S O Tm-Afm Threshold Analysis of Macromolecular Orientation: A Study of the Orientation of Igg and Ige on Mica Surfaces. J. Colloid Interface Sci 1998, 206, 475–481. [PubMed: 9756659]
29. Karsai A; Slack TJ; Malekan H; Khoury F; Lin WF; Tran V; Cox D; Toney M; Chen X; Liu GY Local Mechanical Perturbation Provides an Effective Means to Regulate the Growth and Assembly of Functional Peptide Fibrils. Small 2016, 12, 6407–6415. [PubMed: 27689936]
30. Dicesare PE; Morgelin M; Carlson CS; Pasumarti S; Paulsson M Cartilage Oligomeric Matrix Protein - Isolation and Characterization from Human Articular-Cartilage. J. Orthop. Res 1995, 13, 422–428. [PubMed: 7602403]
31. Engel J; Furthmayr H Electron-Microscopy and Other Physical Methods for the Characterization of Extracellular-Matrix Components - Laminin, Fibronectin, Collagen-Iv, Collagen-Vi, and Proteoglycans. Methods Enzymol. 1987, 145, 3–78. [PubMed: 3600396]
32. Morgelin M; Heinegard D; Engel J; Paulsson M Electron-Microscopy of Native Cartilage Oligomeric Matrix Protein Purified from the Swarm Rat Chondrosarcoma Reveals a 5-Armed Structure. J. Biol. Chem 1992, 267, 6137–6141. [PubMed: 1556122]
33. Hinck AP; Archer SJ; Qian SW; Roberts AB; Sporn MB; Weatherbee JA; Tsang MLS; Lucas R; Zhang BL; Wenker J, et al. Transforming Growth Factor Beta 1: Three-Dimensional Structure in Solution and Comparison with the X-Ray Structure of Transforming Growth Factor Beta 2. Biochemistry 1996, 35, 8517–8534. [PubMed: 8679613]
34. Shi ML; Zhu JH; Wang R; Chen X; Mi LZ; Walz T; Springer TA Latent Tgf-Beta Structure and Activation. Nature 2011, 474, 343–349. [PubMed: 21677751]
35. Josuran R Prot Pi | Protein Tool. https://www.protpi.ch/Calculator/ProteinTool (accessed September 16, 2020).
36. Du Y; Wang Y; Wang L; Liu B; Tian Q; Liu CJ; Zhang T; Xu Q; Zhu Y; Ake O, et al. Cartilage Oligomeric Matrix Protein Inhibits Vascular Smooth Muscle Calcification by Interacting with Bone Morphogenetic Protein-2. Circ. Res 2011, 108, 917–928. [PubMed: 21350216]
37. Gordon KJ; Blobe GC Role of Transforming Growth Factor-Beta Superfamily Signaling Pathways in Human Disease. Biochim. Biophys. Acta, Mol. Basis Dis 2008, 1782, 197–228.
38. Hinck AP Structural Studies of the Tgf-Beta S and Their Receptors - Insights into Evolution of the Tgf-Beta Superfamily. Fed. Eur. Biochem. Soc., Lett 2012, 586, 1860–1870.
39. Scheufler C; Sebald W; Hulsmeyer M Crystal Structure of Human Bone Morphogenetic Protein-2 at 2.7 Angstrom Resolution. J. Mol. Biol 1999, 287, 103–115. [PubMed: 10074410]

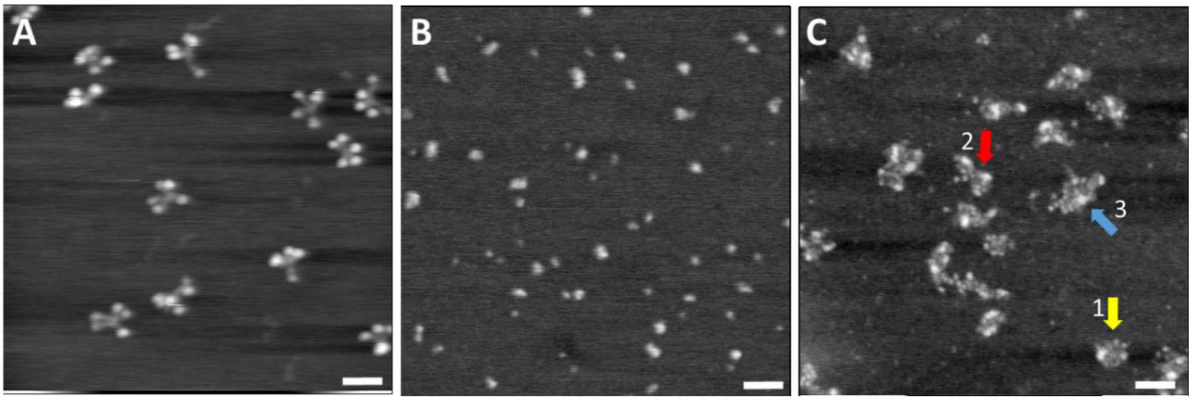

Figure 1.

AFM topographic of protein molecules immobilized on mica(0001) surfaces: (A) COMP molecules, (B) TGF-β1 molecules, and (C) a TGF-β1 and COMP mixture. TGF-β1/COMP complexes adopt geometries such as “sea otter paw” (arrow 1), “butterfly” (arrow 2), and “sting ray” (arrow 3). Tapping mode was used for image acquisition under a speed of 3.5 μm/s, and 1024 x 512 pixels per frame. Scale bar is 50 nm, and height contrast ranges 0 - 2.4 nm.

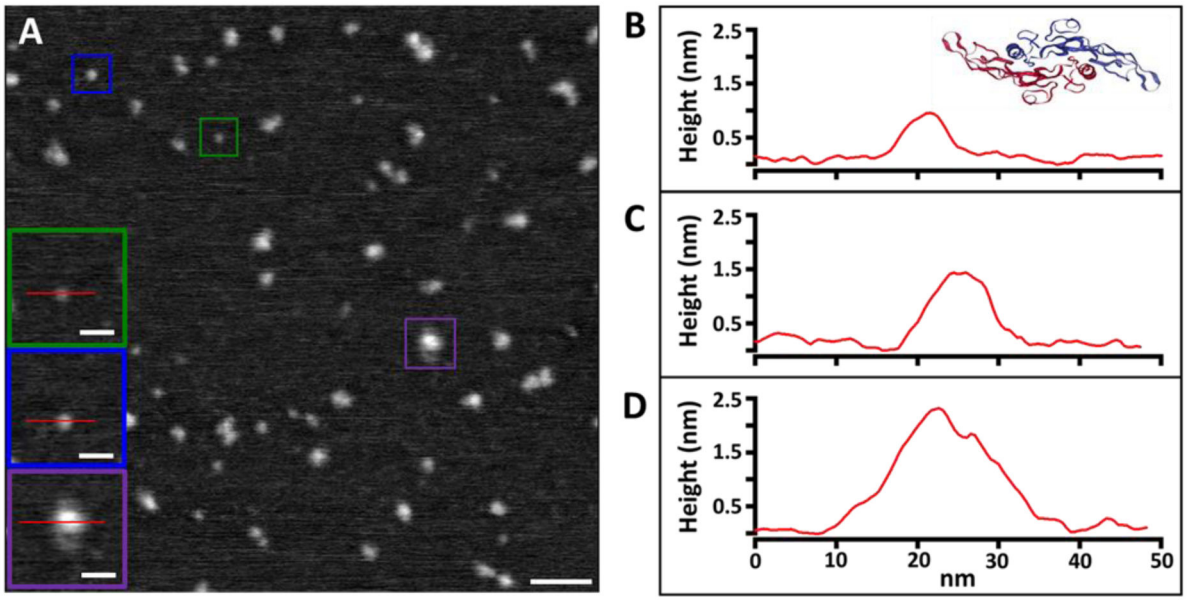

Figure 2.

(A) AFM topographic images of immobilized TGF-β1 molecules on a mica (0001) surface. Scale bar is 50 nm. Insets are the zoom-in views of three characteristic TGF-β1 features as indicated by the green, blue and purple frames, respectively. Inset scale bar = 20 nm. (B), (C) and (D) are the corresponding cursor profiles as indicated in the green, blue, purple insets, respectively. A TGF-β1 homodimer is displayed within the frame of plot (B), based on the known crystal structure (10.2210/pdb1KLD/pdb)

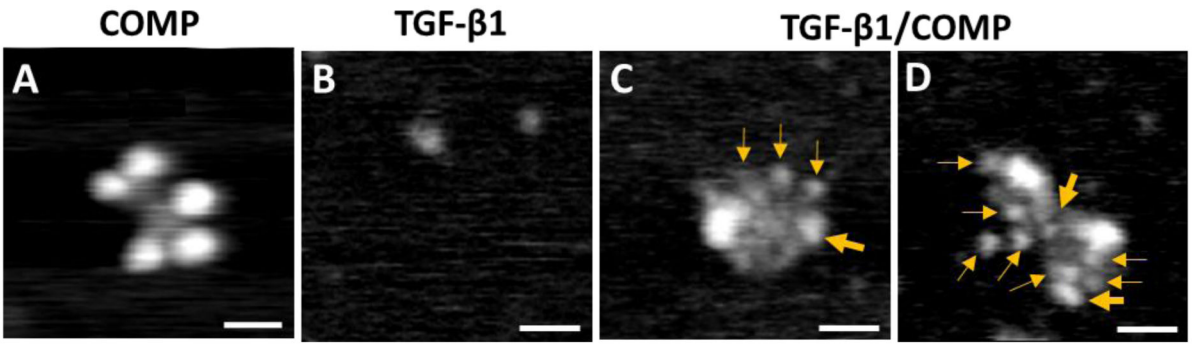

Figure 3.

High-resolution AFM topographic images of representative protein molecules in this investigation: (A) a COMP; (B) a TGF-β1 dimer and a double dimer; (C) a TGF-β1/COMP complex containing one COMP; and (D) a TGF-β1/COMP complex containing two COMP molecules. Yellow arrows point to TGF-β1 molecules within the complex, thin arrows indicate dimeric TGF-β1and thick arrows indicate double dimer TGF-β1. Scale bars = 20 nm.

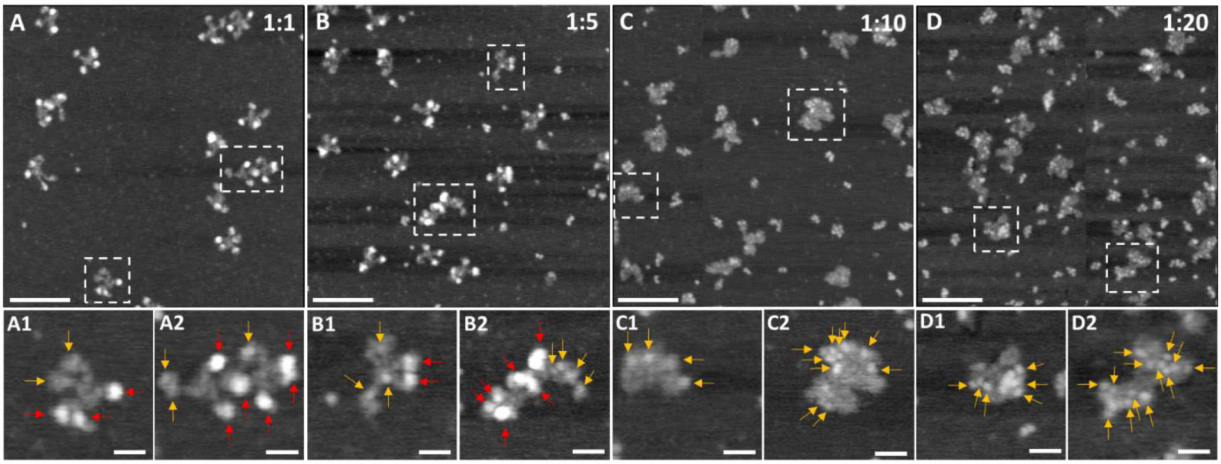

Figure 4.

Top row: AFM topographic images of immobilized TGF-β1 and COMP mixtures at the designed COMP:TGF-β1 ratio as indicated at the top right of each frame. Scale bar = 100 nm. **Bottom row:** Zoom-in views of two representative complexes selected from the frame above, containing one and two COMP molecules, respectively. Red arrows indicate C-terminal domains of COMP and yellow arrows point to the location of the TGF-β1 molecules in the complexes. Scale bar = 20 nm.

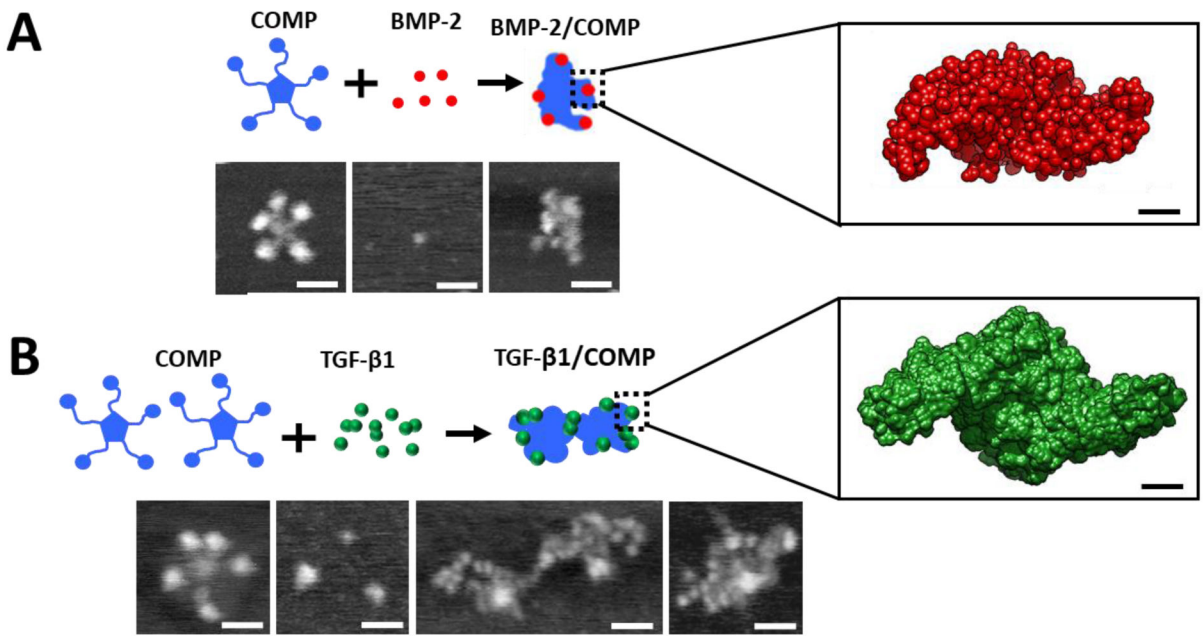

Figure 5.

(A) Schematic diagram of BMP-2 binding with COMP. Corresponding AFM images are shown below. Scale bar among AFM images = 25 nm. (B) Schematic diagram of TGF-β1 binding with COMP. Scale bar among AFM images = 25 nm. The volume filing models of BMP-2 (10.2210/pdb3BMP/pdb) and TGF-β1 (10.2210/pdb1KLA/pdb) are compared. The 3D size of a BMP-2 and TGF-β1 dimer is ~ 7.0 nm x 3.5 nm x 3.0 nm, and ~ 9.0 nm x 4.0 nm x 3.0 nm, respectively. Scale bar among protein models = 1 nm.